Equivalence between Steatite Antennas Spherical Nearfield Test Range and a Typical Far-Field Test Range

I. Introduction

This document is intended as an introduction to our Spherical Near-Field Range (SNFR) facility: describing its capabilities and advantages over more traditional Far-Field systems. This is underpinned with a case study of an AUT (Antenna Under Test) at both the SNFR and an Independent Far-Field range facility; where pattern and gain measurements are compared in an exercise to demonstrate the equivalence between SNFR and Far-Field Range results. Also included is technical overview of the system with further discussion on measurement accuracy.

II. Description

This measurement system was designed and installed by NSI-MI Technologies[1]. The Anechoic Chamber was supplied by Siepel[2] with the absorber installation and overall project managed by Frequensys[3]. The Range is enclosed in a screened anechoic enclosure. Nominal frequency range of operation is 0.5-40GHz. This Range is able to accommodate large dish antennas up to 3m diameter. An antenna of similar size is shown in Fig. 2.

Fig. 1. View from outside our Spherical Near-Field Range.

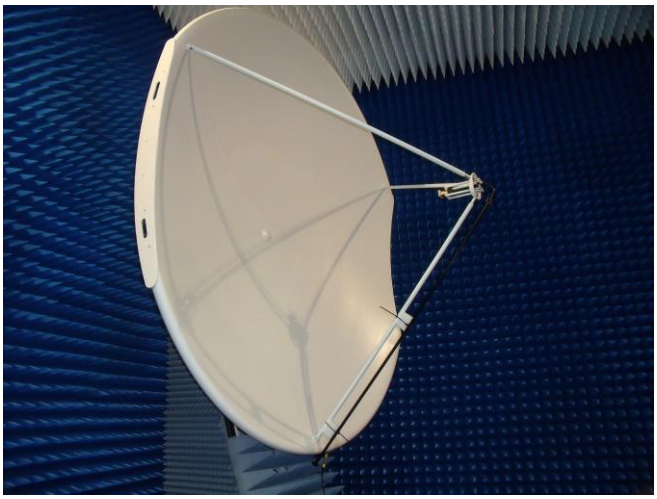

Fig. 2. View inside Chamber showing AUT (2.7m diameter dish).

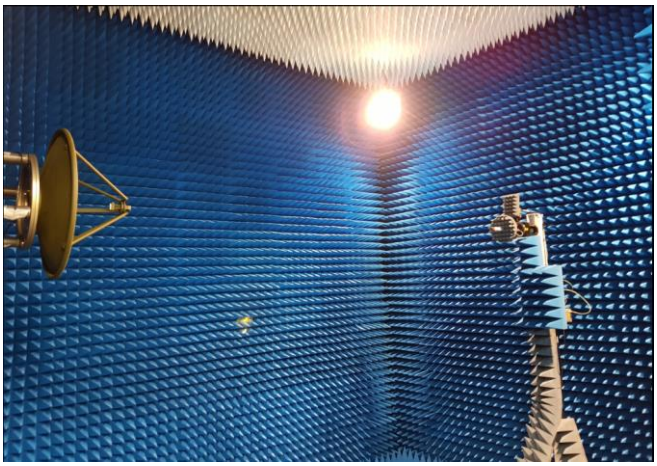

Fig. 3. View inside Chamber showing AUT (0.9m diameter dish) looking towards transmitting probe.

Nominal distance between AUT and Linearly Polarised Probe is (depending on the AUT mount) approximately 4m. Fig. 3 shows Probe as viewed from AUT end. In this picture the AUT is a 0.9m dish.

The AUT rotates in Azimuth (Θ) and Rolls in (ϕ); while the probe (transmitting a swept-frequency signal) rotates between H and V polarisations. (The output data can be converted to Azimuth over Elevation if required). In a single measurement therefore, a 3-dimensional Near-Field pattern of the AUT for each frequency, complete with amplitude and phase for each polarisation component is thus obtained. This data is then processed to produce the Far-Field pattern. More details on the nature of this transform including the specification of the transmitting probe is shown in III.

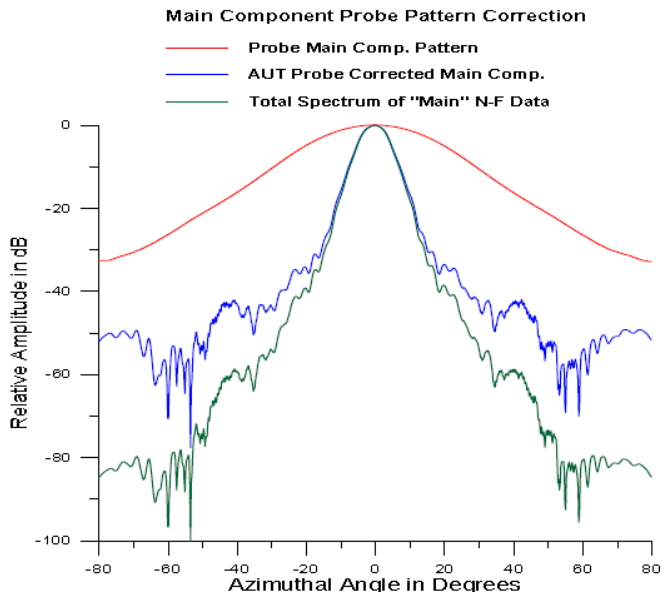

Fig. 4. Effect of the Probe on Far-Field pattern [1]

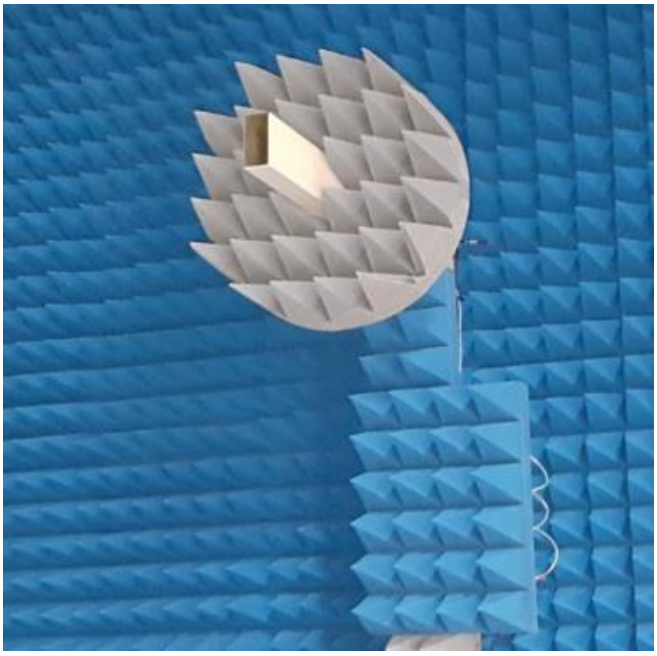

Fig. 5. Picture of OEWG probe and local absorber

III. Near-Far-Field transformation and probe correction

The method used to achieve a Far-Field result is a Fast Fourier Transform (FFT). But the output of this transform needs to be processed further to account for the non-isotropic nature of the probe. This is called probe correction. The basic concept of probe correction is to record the phase and amplitude over a surface in the radiating Near-Field (~3 wavelengths), this is then processed with an FFT to produce Far-Field data (i.e. correction is applied during the Near-Field to Far-Field transformation). The correction, the pattern effect of the probe and the resulting pattern is what would be measured using an ideal probe (Fig. 4).

Probe compensation removes the error associated with non-isotropic probes. The accuracy of the Far-Field result relies on having as small a probe compensation as possible. The probes, therefore, are engineered to have a broad symmetrical beam. These probes are Open Ended Waveguides (OEWG), an example is shown in Fig. 5. Note here the localised absorber: which serves to preserve the symmetry of the beam, by removing interfering effects of back scattering.

In order to maintain the beam quality across frequency the OEWG is narrowband. A broadband (AUT) antenna measurement will require several changes of probe.

An OEWG probe generates a symmetrical low directivity beam which serves to maximise the accuracy of the Near-Far transformation.

IV. Accuracy of Steatite SNFR

NSI-MI[1] carried out several studies to determine the measurement uncertainty of the system[4]. The examples are for Gain (TABLE I.) and Sidelobe (TABLE II.) respectively. Error Figures for each error source Item were determined either by theoretical analysis; or by carrying out repeated measurements. All Error figures were then combined using Root of Sum of Squares (RSS). On the basis of this study, Steatite quote Gain error as: **Gain ±0.22dB.** Likewise, error in sidelobe depth will be **±1.2dB** (based upon the example in VII).

This excludes any uncertainty on the gain standard being used which is dependent upon the accuracy of the gain standard used for any specific measurement. This is often the largest uncertainty in any measurement performed.

TABLE I. Measurement Uncertainty Analysis: Gain [1]

Gain error budget

#	Item	Level (dB)	E/S(dB)
1	Probe relative pattern	0	
2	Probe polarization ratio	0	
3	Probe gain measurement	0.10	-45
4	Probe alignment error	0.0001	-99
5	Normalization constant	0.15	-35
6	Impedance mismatch error	0.10	-27
7	AUT alignment error	0	None
8	Data point spacing (aliasing)	0.01	-60
9	Measurement area truncation	0.01	-60
10	Probe Y position errors	0.001	-79
11	Probe z position error	0.0001	-97
12	Mutual coupling (Probe/AUT)	0.06	-43
13	Receiver amplitude linearity	0.02	-53
14	Systematic phase error	0.0005	-85
15	Receiver dynamic range	0.003	-70
16	Room scattering	0.05	-45
17	Leakage and crosstalk	0.003	-70
18	Random amplitude/phase errors	0.05	-45
	Total (rss)	0.22	-32

TABLE II. MEASUREMENT UNCERTAINTY ANALYSIS: SIDELOBE [1]

Sidelobe error budget (-30 dB sidelobe)

#	Item	Level (dB)	E/S (dB)
1	Probe relative pattern	0.04	-47
2	Probe polarization ratio	0	None
3	Probe gain measurement	0	None
4	Probe alignment error	0.02	-73
5	Normalization constant	0	None
6	Impedance mismatch error	0	None
7	AUT alignment error	0	None
8	Data point spacing (aliasing)	0.15	-35
9	Measurement area truncation	0.3	-30
10	Probe Y position errors	0.03	-49
11	Probe z position error	0.15	-35
12	Mutual coupling (Probe/AUT)	0.80	-20
13	Receiver amplitude linearity	0.15	-35
14	Systematic phase error	0.09	-40
15	Receiver dynamic range	0.48	-25
16	Room scattering	0.80	-20
17	Leakage and crosstalk	0.15	-35
18	Random amplitude/phase errors	0.03	-45
	Total (rss)	1.2	-17

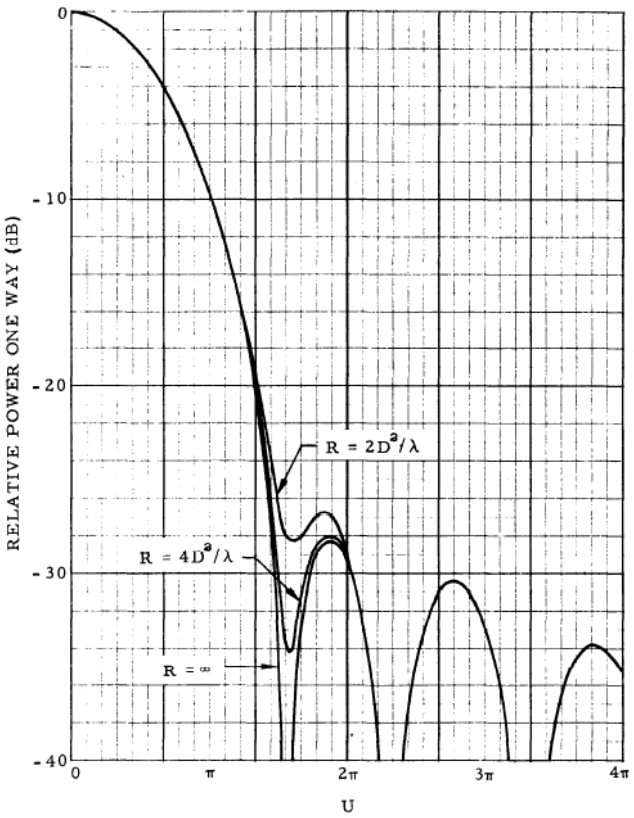

Fig. 6. Effect of range distance on resolution of main beam [7]

V. INACCURACY OF A FAR-FIELD TEST RANGE

It is a common misconception that an antenna test range conforming to $2D^2/\lambda$ (or Rayliegh Range, where D is aperture of AUT) produces accurate Far-Field measurements. However, this is not true as the wave front even at this distance is not plane but spherical, resulting in a phase taper across the receiving aperture. Indeed, at $4D^2/\lambda$ there is still a phase taper of λ/32 or 10°[5],[6].

Further studies revealed a corresponding impact on the shape of the nominal Far-Field patterns, namely in the depth of the first null [6]. It is only at distances much greater than $8D^2/\lambda$ that the depth of the null and therefore the true Far-Field characteristics of the beam can approach resolution. Infinity is the only point where the Far-Field pattern can be fully resolved.

A Far-Field range, therefore cannot realistically deliver an accurate Far-Field pattern. Furthermore, in addition to this intrinsic limitation; Far-Field range data will be further influenced by ground reflections, RF interference and environmental factors. Factors that will not be present in an indoor, screened and anechoically lined test chamber.

Steatite Antennas Spherical Nearfield Range (SNFR) can measure Far-Field at infinity by acquiring a 3D antenna pattern measurement in the Nearfield (Or the Fresnel zone: where the wave fronts are still circular); and using FFT and Spherical Mode Expansion algorithm to transform to the true Far-Field. A full presentation of this method including mathematical summary, test requirements and further references can be found in [8].

VI. SNFR SUMMARY OF FACTS

The following section briefly summarises the advantages of a SNFR.

Full 3D pattern acquisition in a single measurement: No need to set up for specific pattern cuts and polarisations. All data required to generate Far-Field co-polar, cross-polar or indeed any arbitrary polarisation component and pattern cut is captured in the Near-Field measurement.

More accurate than traditional Far-Field range. Our system transforms raw measurement data beyond 2D2/λ to infinity; thus, removing any residual Near-Field influence (especially in sidelobes) that can persist even at the Rayleigh Range.

Diagnostic capability: Our system has the ability to take a 3D Far-Field pattern profile and “back transform” to the radiating surface of the Antenna Under Test (AUT); to show amplitude & phase profiles that could be source of Far-Field pattern anomalies.

Extended capability at high frequencies: By application of Distributed signal mixing. All RF signals are mixed down to IF using mixing units located close to the antennas, thereby reducing signal loss in cables upholding signal to noise quality and maintaining measurement accuracy.

Extended capability at low frequencies: by the application of Mathematical Absorber Reflection Suppression (MARS) technology that effectively gates out wall reflections; means the SNFR capability is not compromised by limitations in chamber absorber performance.

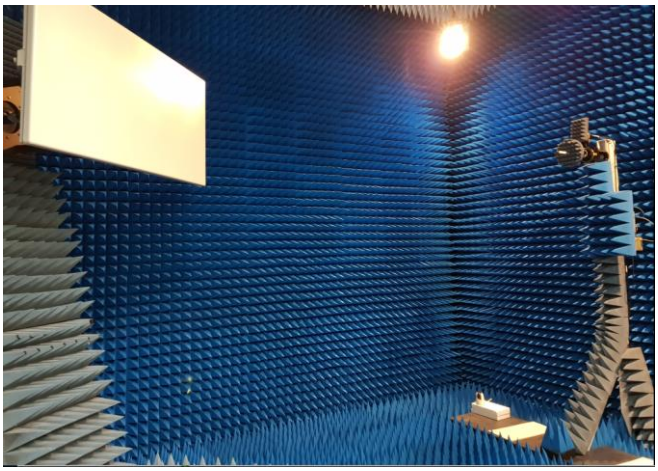

Fig. 7. Planar Array Antenna mounted in SNFR

Fig. 8. Planar Array Antenna mounted on the Independent Far-Field range

VII. Case Study: Comparing SNFR with Far-Field Range

This section compares results from the Steatite Antennas SNFR to those from an Independent Far-Field Range Facility for the **same** antenna.

A. AUT in the Steatite Antennas SNFR

The AUT was a 1.5m x 0.7m planar array antenna (operating at 3 GHz). The range distance of the SNFR was approximately 3.5m, therefore placing the SNFR data acquisition within the Near-Field (Rayleigh distance 45m). This is an ideal configuration to apply and assess the accuracy of the near-Far-Field transformation. The SNFR configuration with the AUT in question is shown in (Fig. 7). Note the small distance between AUT and Probe.

B. AUT at the Independent Far-Field Range

This outdoor range was 500m in length; or 11 x Rayleigh range; Therefore, making this a good approximation to an infinite Far-Field. A view looking down range from the AUT is shown in (Fig. 8). The transmitting probe is at the far end of the field.

C. Results and Analysis

Measurements from each facility were normalised for amplitude and overlaid on Cartesian axes. The data output from each facility did not share a common format. Both sets of data therefore, were imported into Excel.

1) Comparing Patterns

Fig. 9 and Fig. 10 show normalised Azimuth and Elevation radiation pattern for both test ranges.

Note the good correlation between SNFR and Far-Field Range. Patterns appear equivalent. Some minor differences become evident when zooming in on main beam (Fig. 11 and Fig. 12).

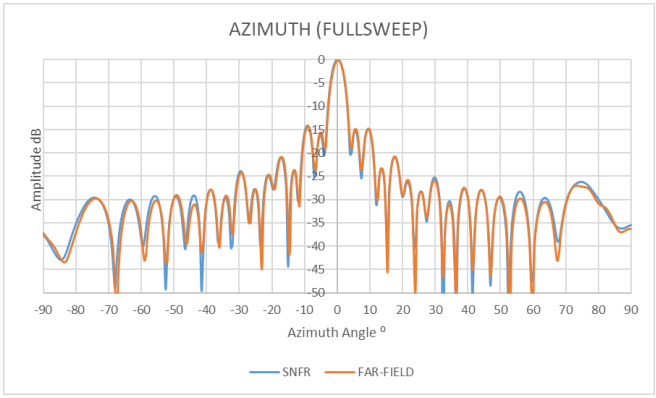

Fig. 9. Far-Field plot comparing SNFR and Far-Field results (full range): Azimuth

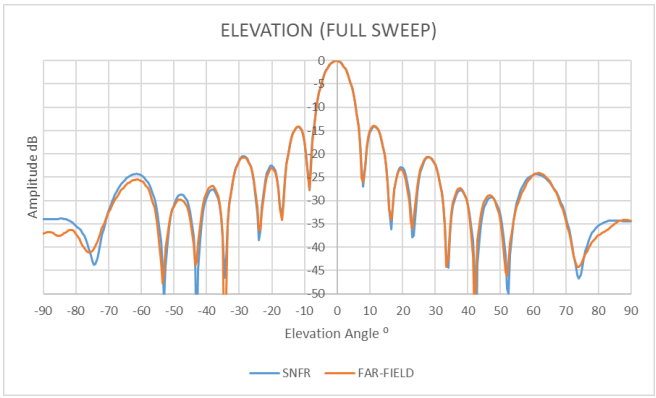

Fig. 10. Far-Field plot comparing SNFR and Far-Field results (full range): Elevation

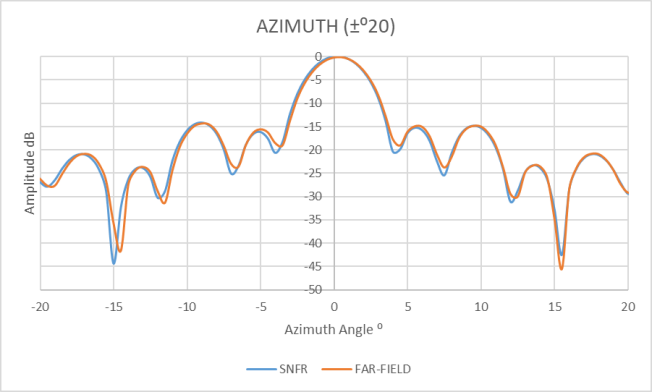

Fig. 11. Far-Field plot comparing SNFR and Far-Field results (±20°): Azimuth

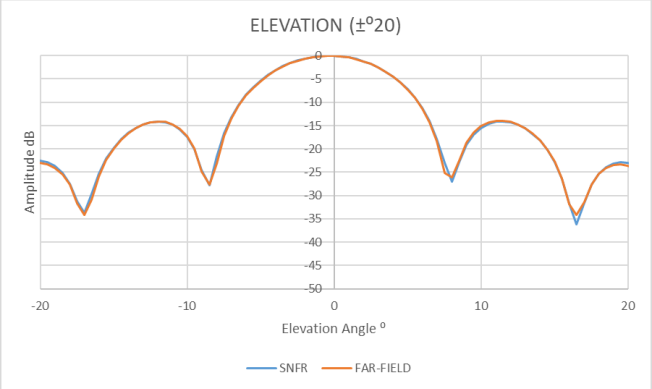

Fig. 12. Far-Field plot comparing SNFR and Far-Field results (±20°): Elevation

Fig. 11 and Fig. 12 plots were further computed over ±5° to give difference in Relative Amplitude between SNFR and Far-Field Facility (Fig. 13 and Fig. 14).

These differences can be put down to the following:

1. Far-Field range distance is still finite; causing SNFR nulls to be generally deeper.
2. Differing cross-polar performance of the respective measurement probes: The SNFR probes are OEWG, optimised for optimum cross-polar performance.
3. Alignment in Azimuth Origin: Highlighted in Fig. 13. This is more likely to originate from the Far-Field facility as Az and El were acquired as two separate acquisitions leaving possibility of mechanical inaccuracies between measurements.
4. In the SNFR the measurement tower is lined with RAM, this is something not present within the Far-Field range example (Fig. 7 and Fig. 8).

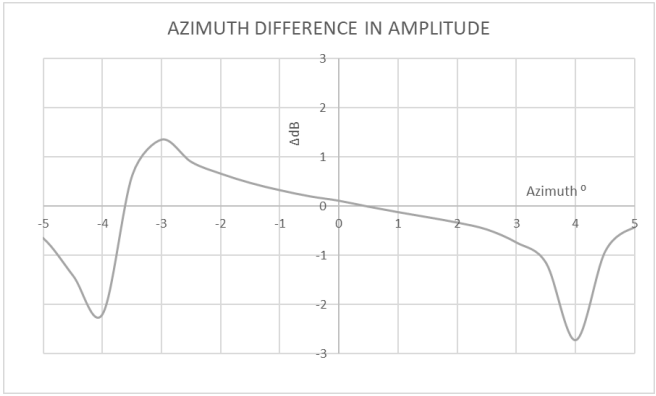

Fig. 13. Difference in Amplitude for SNFR Vs. Far-Field Range (±5°): Azimuth

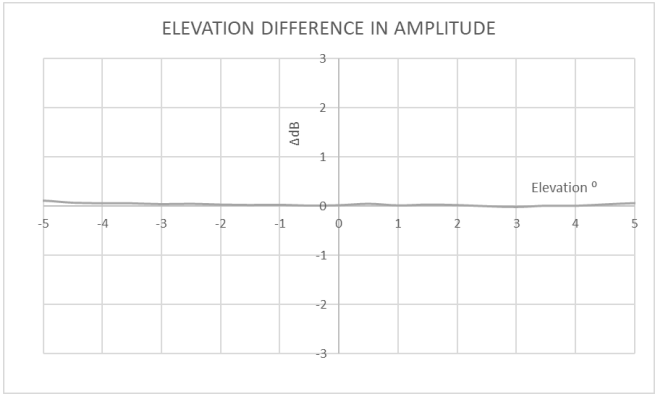

Fig. 14. Difference in Amplitude for SNFR V Far-Field Range (±5°): Elevation

2) Comparing Gain

TABLE III. summarises the gain measured at each site. In both instances a Gain Reference Measurement was performed using local gain standards.

Examining the measured gains and comparing the respective measurement uncertainties confirms that gain results are equivalent.

TABLE III. GAIN RESULTS (WITH UNCERTAINTY) FROM STEATITE SNFR AND INDEPENDENT FAR-FIELD RANGE FACILITY

Measurement Facility	Measured Gain at 3GHz dBi	Uncertainty ±dB
Steatite SNFR	28.3	0.22[1]
Independent Far-Field Range Facility	28.7	0.5[2]

[1] As shown in IV

[2] *Figure supplied by Independent Far-Field Range Facility Management*

VIII. Data Output Format from SNFR

The following plots display the same transformed Far-Field output as discussed in VII. The Output Graphic User

Interface (GUI) provided by NSI-MI can present data in several formats – Cartesian, Polar, 2D (Fig. 16) and 3D (Fig. 15).

IX. Conclusion

A case study of a Planner Array Antenna measured using the SNFR produces almost identical patterns to those generated for the same antenna measured on an Independent Far-Field Range. Any minor differences can be explained by measurement uncertainties or mechanical drift. Moreover, the Gains from the SNFR and the Far-Field facility are the same (within measurement uncertainty).

For the SNFR, the dimensions and operating frequency of the AUT placed the measurement well within the Near-Field as defined by the Rayleigh Range. For this range to produce the same result as a Far-Field Facility over an order of magnitude beyond Rayleigh validates the effectiveness of the SNFR and demonstrates equivalence in performance between Steatite SNFR and a Far-Field Test Range.

Furthermore, this document cites Academic research that exposes the inherent inaccuracy of shorter Far-Field ranges that rely on Rayleigh Range criteria. The only way to guarantee an accurate measurement is to measure at infinity with Spherical Nearfield Range technology or use a very large Far-Field Range.

The technology around the Spherical Nearfield Range has been rigorously researched and is a standard Antenna measurement technique widely used across industry including Aerospace, Defence, Automotive and Satellite.

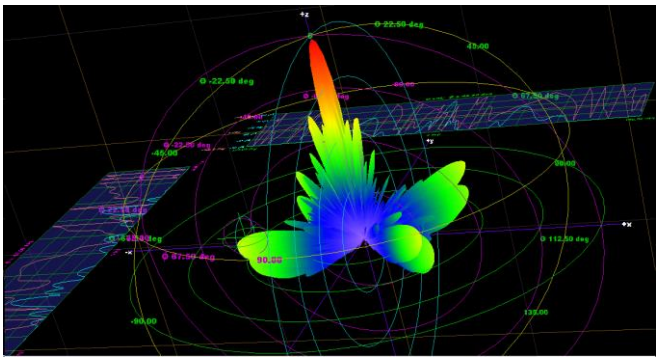

Fig 15: SNFR Data Output Format: 3D Far-Field plot

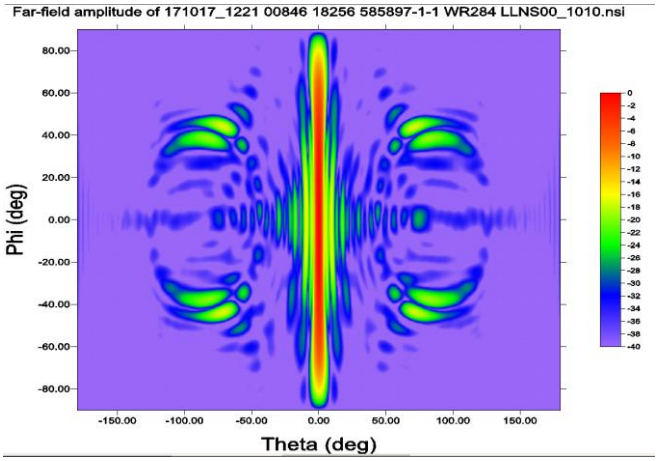

Fig 16: SNFR Data Output Format: 2D Image Far-Field plot

References

[1] https://www.nsi-mi.com
[2] https://www.siepel.com/
[3] http://www.frequensys.co.uk/
[4] NSI-MI Technologies, "Short Course: Near-Field Antenna Measurements," March 2017.
[5] Jack B Chastain et al, "Investigation of Precision Pattern Recording and Display Techniques," RADC-TDR-63-247; AD 415912: April 1963.
[6] R. C Hansen, "Tables of Taylor Distributions for Circular Aperture Antennas, "IRE Transactions on Antennas and Propagation: Jan 1960.
[7] D.R. Rhodes, "On Minimum Range for Radiation Patterns,"Proc. IRE, Vol 42, No 9, pp 1408-1410: September 1954.
[8] C. Parani, S. Gregson, J McCormick, D Janse van Rensburg "Theory and Practice of Modern Antenna Range Measurements", Chapter 7: Spherical nearfield antenna measurements. ISBN 978-1-84919-560-7

STEATITE LIMITED (ANTENNAS)
UNIT 15 CROFT BUSINESS PARK
SOUTHERN AVENUE
LEOMINSTER
HEREFORDSHIRE
HR6 0QF

STEATITE LIMITED (HEADQUARTERS)
RAVENSBANK BUSINESS PARK
ACANTHUS ROAD
REDDITCH
WORCESTERSHIRE
B98 9EX

WWW.STEATITE.COM
A SOLID STATE GROUP COMPANY
Telephone: +44 (0)1568 617920
Fax: +44 (0)1568 612138
Email: sales.antennas@steatite.co.uk